Multicomponent anion exchange simulation of phosphate removal and recovery from municipal wastewater using Aspen Adsorption

Davide Pinelli, Benedetta Martellotti, Elisa Girometti, Laura Bernacchioni, Giacomo Antonioni, Valerio Cozzani, Dario Frascari

SUPPLEMENTARY MATERIAL

Text S1. Kinetic tests: operational conditions, simulation and results

The tests were carried out with the actual WW, at 22°C, in an orbital shaker set at 160 rpm with an initial concentration of 30 mgP L^{-1}. The sorbent was in granulated form with the same mesh used in the BT tests (0.355 – 0.710 mm size). Experimental data are plotted in Figure S3 in terms of sorbed concentration versus time.
The kinetic experimental data can be used to gain information about the rate limiting step of the adsorption process. 4 different steps are involved in the adsorption form the liquid phase to the surface of the sorbent: i) external film mass transfer, ii) diffusion in the pore structure of the sorbent, iii) adsorption on the active sites of the sorbent, iv) superficial diffusion in the surface of the pore of the adsorbate.
Experimental data were interpolated by non-linear least squares using the following three models:

1) Pseudo-first-order (PFO) model, or external film mass transfer:

$$C_S(\mathrm{t}) = C_{S,eq}\,(1 - e^{k_1 t}) \qquad \text{(Eq. S1)}$$

where $C_{S,eq}$ (mg g^{-1}) and C_S (mg g^{-1}) are the amounts of adsorbate sorbed per mass of adsorbent at equilibrium and at any time *t* (min), respectively; and k_1 (min^{-1}) is the rate constant of the PFO equation.

2) Pseudo-second-order (PSO) equation:

$$C_S(t) = \frac{C_{S,eq}^2\, k_2 t}{1 + C_{S,eq} k_2 t} \qquad \text{(Eq. S2)}$$

where $C_{S,eq}$ (mg g^{-1}) and C_S (mg g^{-1}) are the amount of adsorbate sorbed at equilibrium and at any time *t* (min), respectively; and k_2 (g/(mg min)) is the rate constant of the PSO equation.

3) Weber–Morris model, or intra-particle diffusion model:

$$C_S(\mathrm{t}) = k_{IP}\, t^{0.5} + C \qquad \text{(Eq. S3)}$$

where C_S (mg g^{-1}) is the amount of adsorbate adsorbed at any t (min) and k_{IP} (mg g^{-1} $min^{-0.5}$) is the rate constant.

The best-fitting curves are shown in Figure S3 together with the experimental data.
The PFO and PSO models resulted in very low interpolation quality, indicating that superficial area is not the rate-limiting step and that transport phenomena influence the sorption performance.
The Webber-Morris intra-particle diffusion and external film transfer model provided a satisfactory data interpolation, with a 95% R^2. The good performance of Weber–Morris model suggests the intraparticle diffusion is involved in the rate-limiting step. However, the presence of a non-null intercept in the plot of C_S against $\sqrt{t}$ suggests that the external film mass transfer is involved as well

(data not shown; Tran et al., 2017, Mistakes and inconsistencies regarding adsorption of contaminants from aqueous solutions: A critical review. Water Research, 120, 88-116). This is not surprising, as orbital agitation during the kinetic test was relatively mild, to prevent granule disaggregation by attrition.

Figure S3 shows that, after 5 minutes, the P sorbed concentration was equal to 40-50% of the long-term value achieved after 4 hours. This outcome indicates that P sorption on the pyroaurite granules is a rapid phenomenon, and that the 5-min EBCT chosen for the adsorption tests is a suitable value.

Text S2. Calculation of the adsorption operating capacity relative to each anion *i*

The operating capacity at the breakpoint, BP, can be defined as:

$$operating\ capacity\ (OC)\ @\ BP = \frac{mass\ i\ adsorbed\ @\ BP}{mass\ of\ dry\ sorbent}$$

The mass of compound i adsorbed can be calculated by integration of the experimental breakthrough curve:

$$m_{i,adsorbed,BP} = m_{i,fed}(t_{BP}) - m_{i,outlet}(t_{BP}) = Q \cdot \int_0^{t_{BP}} C_{i,inlet} \cdot dt - Q \cdot \int_0^{t_{BP}} C_{i,outlet} \cdot dt$$

$$= Q \cdot C_{i,L0} \cdot t - Q \cdot \int_0^{t_{BP}} C_{i,outlet} \cdot dt$$

In this approximated approach, the mass of i present in the liquid inside the column is neglected.

Text S3. Literature-based assessment of the theoretical mass-transfer coefficients relative to phosphate, chloride, bicarbonate and sulphate

A theoretical evaluation of the MTC was performed for all the simulated anions (phosphate, chloride, bicarbonate and sulphate) based on correlations commonly used in the literature.
Two different in-series types of mass transport are involved in adsorption: i) mass transport from the bulk of the liquid to the surface of the particle (external film mass transport), and ii) mass transport in the pores (diffusion in the pores).

i) External mass transport from the bulk of the liquid to the surface of the particle

Mass transport from the bulk of the liquid to the external surface of the particle is commonly described by the equation:

$$m''_{i,ext} = k_{i,f} \cdot (C_{i,L,bulk} - C_{i,L,ext})$$

Where: $m''_{i,ext}$ is the mass flow of adsorbate i transferred from the bulk of the liquid to the external surface of the sorbent, $k_{i,f}$ the mass transfer coefficient of anion i, $C_{i,L,bulk}$ the concentration in the bulk of the liquid solution, $C_{i,L,ext}$ is the concentration at the external solid surface (at the entrance of the pore).
The $k_{i,f}$ values for the four simulated anions were estimated using dimensionless correlations of Sherwood number against the Reynolds and Schmidt numbers.
The Reynolds number for the particle was calculated according to the following definition:

$$Re = \frac{\rho \cdot v_s \cdot d_p}{\mu}$$

where ρ e μ are the density and viscosity of the liquid, d_p the (mean) particle diameter, and v_s the superficial velocity of the liquid. In the actual breakthrough operating conditions of the present work Re is always less than 1.
The Schmidt number is defined as:

$$Sc = \frac{\mu}{\rho \cdot D_{i,L}}$$

where $D_{i,L}$ is the molecular diffusivity of the adsorbate i in the liquid.
Finally, the Sherwood number is defined as:

$$Sh = \frac{k_{i,f} \cdot d_p}{D_{i,L}}$$

For the Sh assessment, the Kataoka et al. (1972) correlation was selected, as it refers to the correct Re range for the operational conditions of this work:

$$Sh = 1.85 \cdot \left(\frac{1-\varepsilon}{\varepsilon}\right)^{0.33} \cdot Re^{0.33} \cdot Sc^{0.33}$$

where ε is the total porosity. It is valid for $Re < 40$.
Two further correlations were tested, and gave similar results:
Wakao and Funazkri (1978):

$$Sh = 2 + 1.1 \cdot Re^{0.6} \cdot Sc^{1/3}$$

valid for $3 < Re < 1000$.

Wilson and Geankoplis (1966):

$$Sh = \frac{1.09}{\varepsilon} \cdot Re^{0.33} \cdot Sc^{0.33}$$

Valid for $0.0015 < Re < 55$.

The external surface-based mass transfer coefficient $k_{i,f}$ was thus calculated as:

$$k_{i,f} = \frac{Sh \cdot D_{i,L}}{d_p}$$

The corresponding external volumetric mass-transfer coefficient referred to the bed volume was assessed as:

$$MTC_{i,ext} = \frac{6 \cdot k_{i,f} \cdot (1 - \varepsilon_{ip})}{d_p}$$

where ε_{ip} is the inter-particle porosity.

ii) Internal diffusion in the pores

The internal diffusive transport in the pores is commonly described by the Fick diffusion equation:

$$m''_{i,int} = -D_{i,e} \cdot \frac{dC_{i,L}}{dx}$$

where: $m''_{i,int}$ is the mass flow of adsorbate i transferred inside the pore volume, $D_{i,e}$ the effective diffusion coefficient in the porous medium, $C_{i,L}$ the concentration in the liquid solution in the pore, and x the longitudinal spatial coordinate in the pore.

$D_{i,e}$ values for all the anions were calculated from the corresponding diffusivities, D_L, which were database found in the literature (Parkhurst and Appelo, 2013; Vanýsek, 1992). Then the D_e is calculated using the well-known equation:

$$D_{i,e} = \frac{\varepsilon_P \cdot D_{i,L}}{\tau}$$

where ε_P in the internal porosity of the solid (pore volume / particle volume) and τ is the pore tortuosity (generally estimated between 1.5 and 5). Tortuosity was estimated as a function of the porosity using two different equations, which gave similar results:

Wakao and Smith, 1962:

$$\tau \cong \frac{1}{\varepsilon_P}$$

Suzuki and Smith, 1972:

$$\tau \cong \varepsilon_P + 1.5 \cdot (1 - \varepsilon_P)$$

The corresponding internal volumetric mass-transfer coefficient was assessed as:

$$MTC_{i,int} = \frac{60 \cdot D_{i,e} \cdot (1 - \varepsilon_{ip})}{d_p^2}$$

The combined volumetric mass-transfer coefficient MTC_i referred to the bed volume was thus calculated as:

$$MTC_i = \frac{1}{\frac{1}{MTC_{i,ext}} + \frac{1}{MTC_{i,int}}}$$

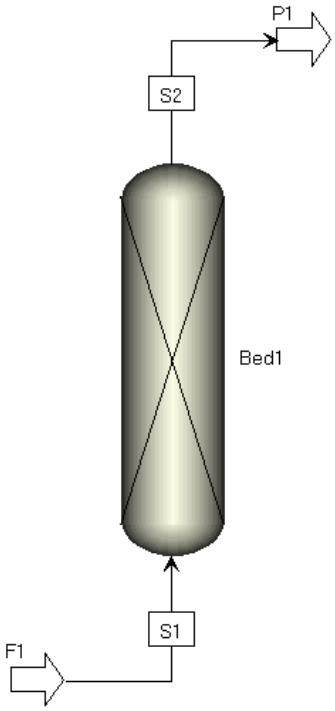

Figure S1. Flowsheet set in Aspen Adsorption to simulate the adsorption tests.

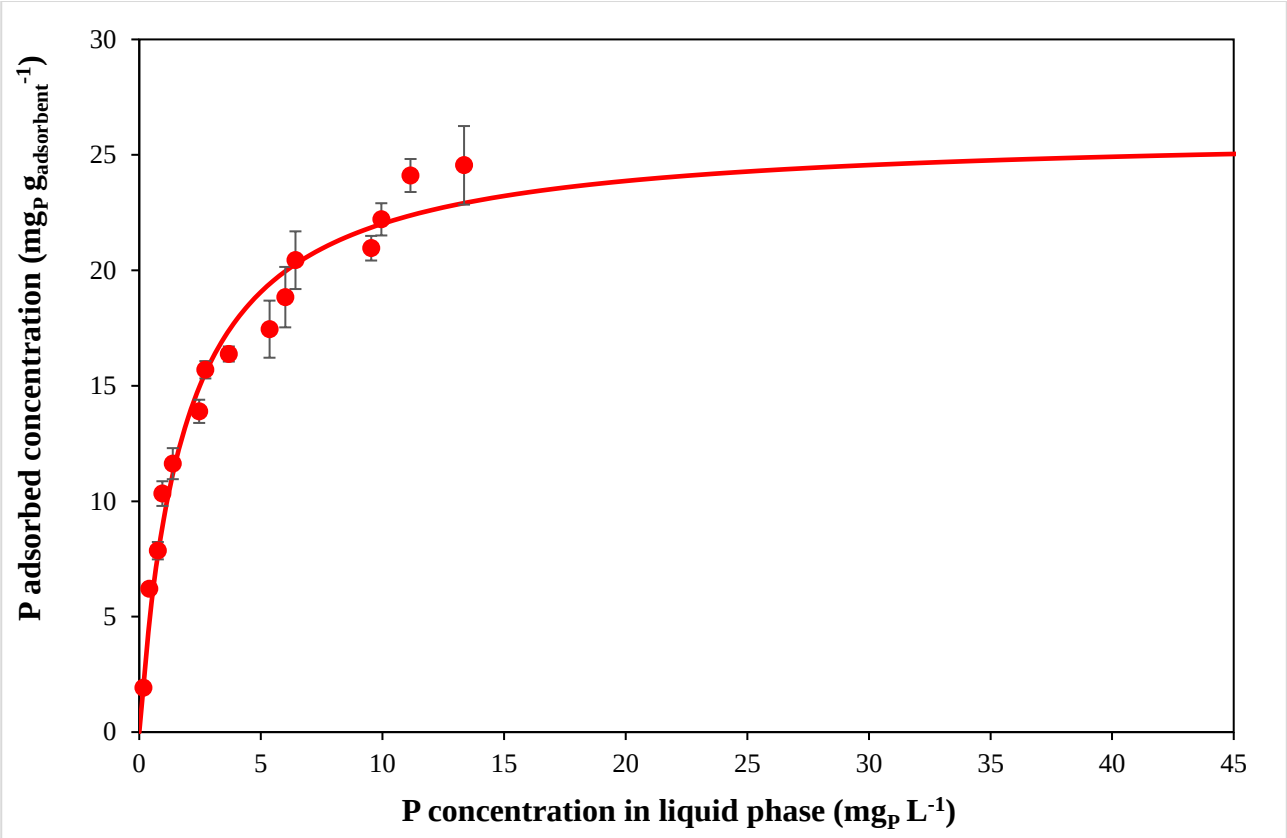

Figure S2. P adsorption isotherm conducted with virgin calcined pyroaurite, using the Bologna WWTP effluent. The best-fitting Langmuir interpolation is shown as a solid line.

Langmuir model: $C_{S,eq} = \frac{C_S^{\infty} \cdot C_{L,eq}}{\frac{1}{K_{eq}} + C_{L,eq}}$

where: $C_{S,eq}$ ($mg_P/g_{dry\ sorbent}$) and $C_{L,eq}$ (mg_P/L) indicate respectively the amount of sorbed P per unit mass of adsorbent and the P concentration in the liquid phase at equilibrium; C_S^{∞} ($mg_P/g_{dry\ sorbent}$) the maximum amount sorbed per unit mass of adsorbent, corresponding to a complete monolayer on the adsorbent surface; $K_{eq,}$ ($L_{pore\ volume}/mg_P$) the constant related to the affinity between the binding sites and P.

The resulting best-fitting parameters are: C_S^{∞} = 26 ± 2 $mg_P/g_{dry\ sorbent}$; K_{eq} = 0.55 ± 0.15 $L_{pore\ volume}/mg_P$.

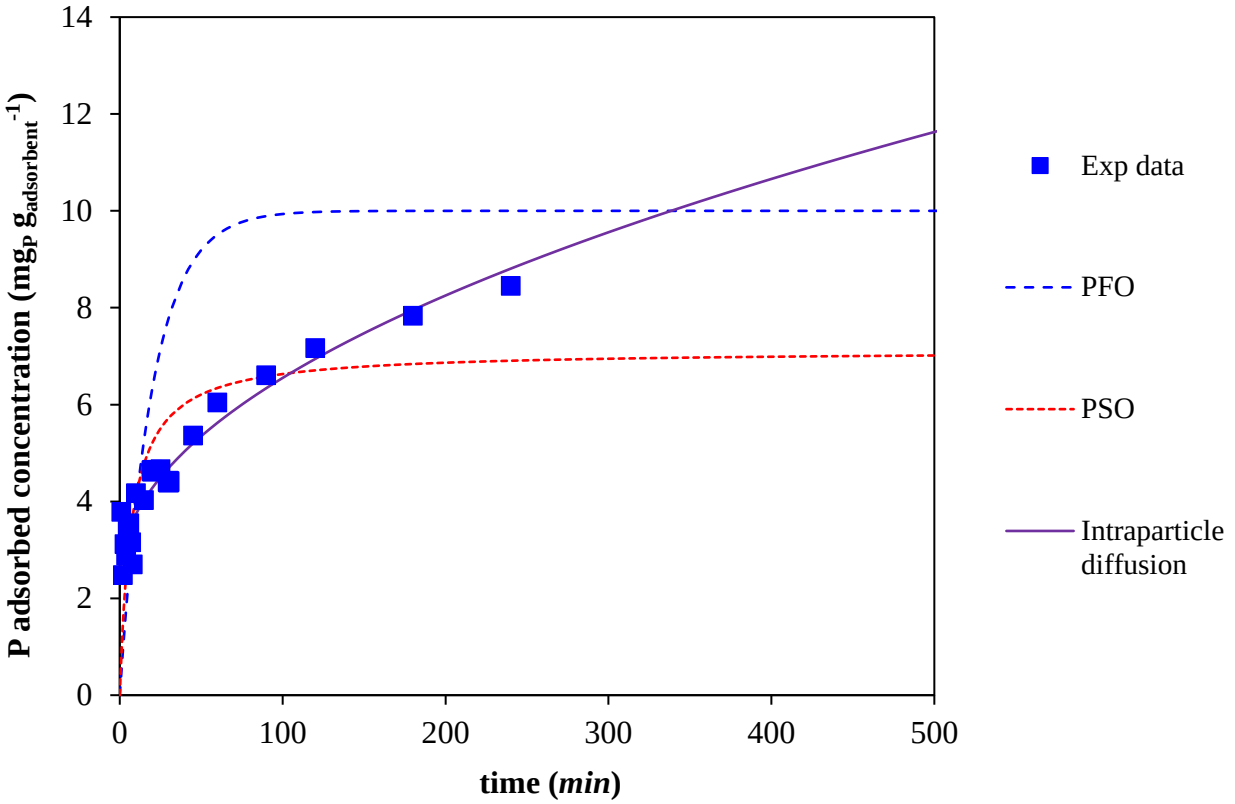

Figure S3. Kinetic test performed with calcined pyroaurite. The best-fitting interpolations obtained with the pseudo-first order model (PFO), the pseudo-second order model (PSO) and the Weber–Morris intra-particle diffusion model are shown, in addition to the experimental data.

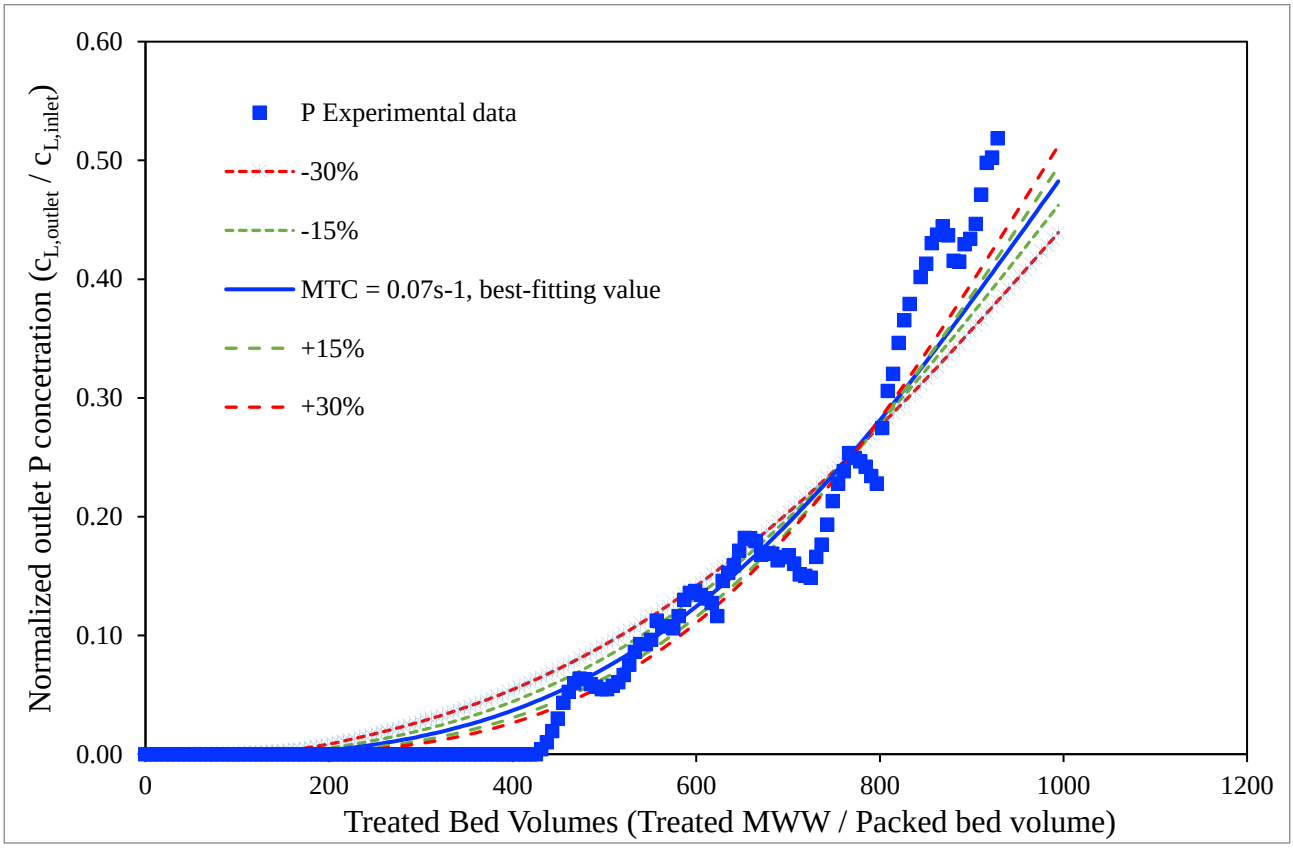

Figure S4. Sensitivity of the P adsorption model to variations of the average $\overline{MTC}$: simulated phosphate adsorption curves obtained with $\overline{MTC}$ = 0.07 s^{-1}, which resulted the optimal value, with a ± 15% $\overline{MTC}$ variation (green dashed curves) and with a ± 30% $\overline{MTC}$ variation (red dashed curves). The experimental curve relative to test BT-a is shown with blue squares. Concentrations are normalized by the average feed concentration of phosphate, equal to 7 mg_P L^{-1}.

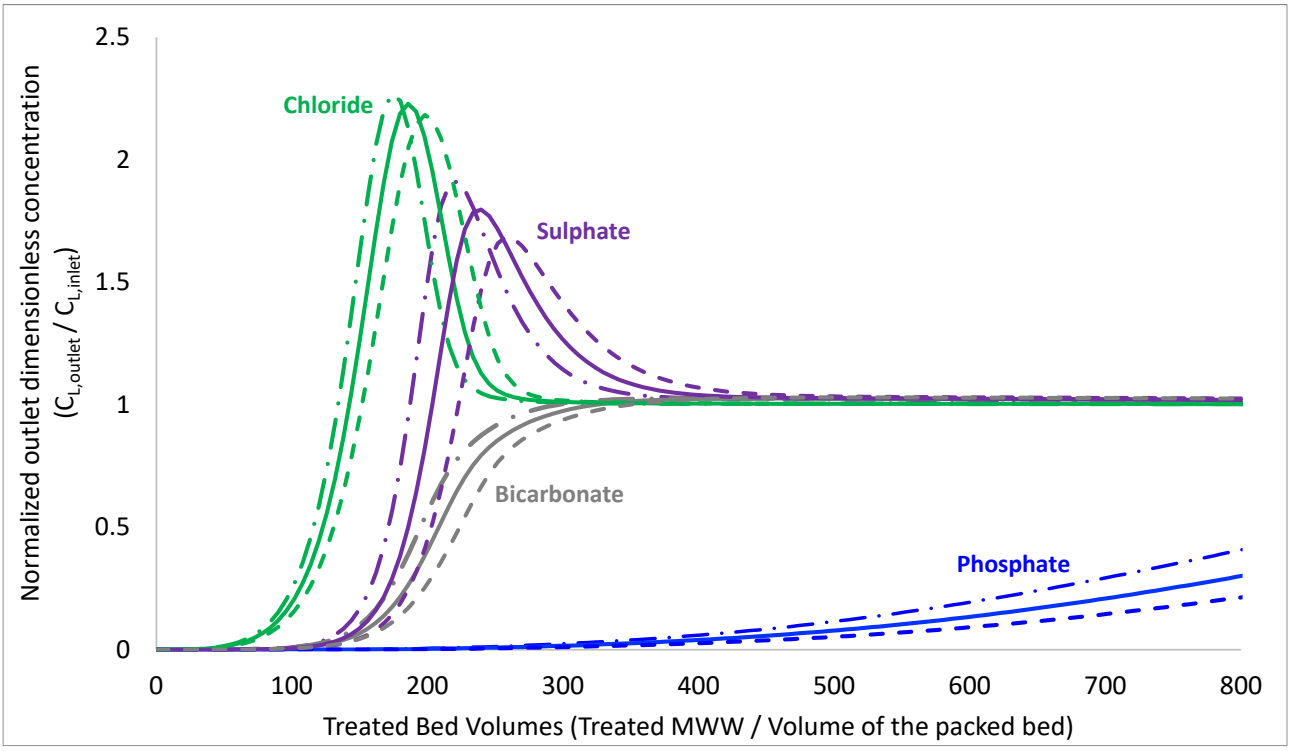

Figure S5. Simulated outlet dimensionless concentrations of all anions, obtained with the model parameters reported in Tables 2 and 3, imposing a -10% and a +10% variation of the inlet bicarbonate concentration reported in Table 1. For each anion, the continuous line refers to the benchmark condition (bicarbonate inlet concentration equal to the values reported in Table 1), the dashed line (- - - - -) refers to the -10% variation in inlet bicarbonate level, and the semi-dashed line (— · — · — refers to the +10% variation in inlet bicarbonate level. Concentrations are normalized by the average feed concentrations: phosphate 7 mg_P L^{-1}, chloride 150 mg L^{-1}, sulphate 104 mg L^{-1}, bicarbonate 615 mg L^{-1} ± 10%.

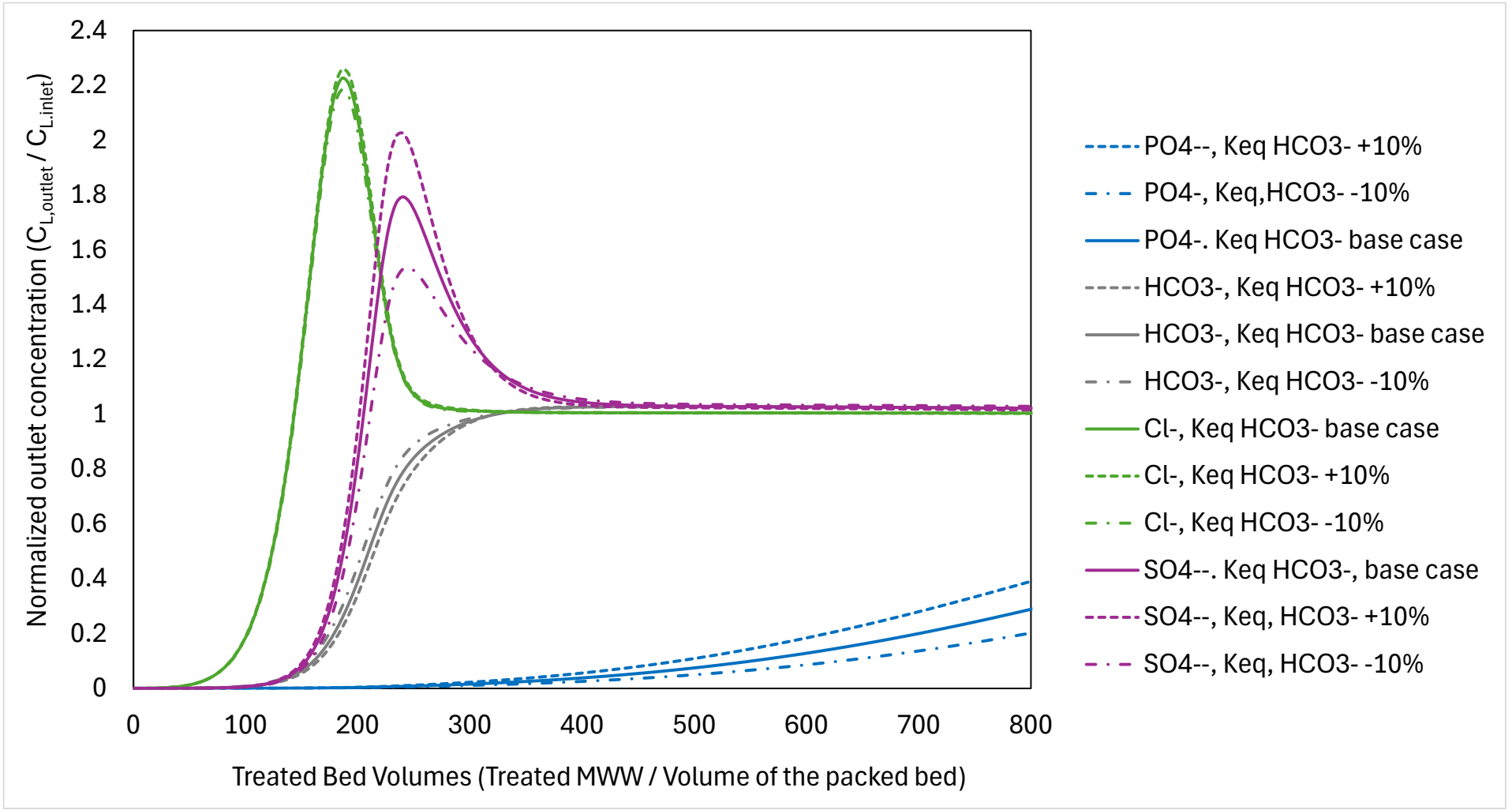

Figure S6. Simulated outlet dimensionless concentrations of all anions, obtained with the model parameters reported in Tables 2 and 3, imposing a -10% and a +10% variation of the bicarbonate equilibrium constant reported in Table 2. For each anion, the continuous line refers to the benchmark condition ($K_{HCO3,OH}$ = 9.3), the dashed line (- - - - -) refers to the +10% variation in $K_{HCO3,OH}$, and the semi-dashed line (— · — · —) refers to the -10% variation in $K_{HCO3,OH}$. Concentrations are normalized by the average feed concentrations: phosphate 7 mg_P L^{-1}, chloride 150 mg L^{-1}, sulphate 104 mg L^{-1}, bicarbonate 615 mg L^{-1}.

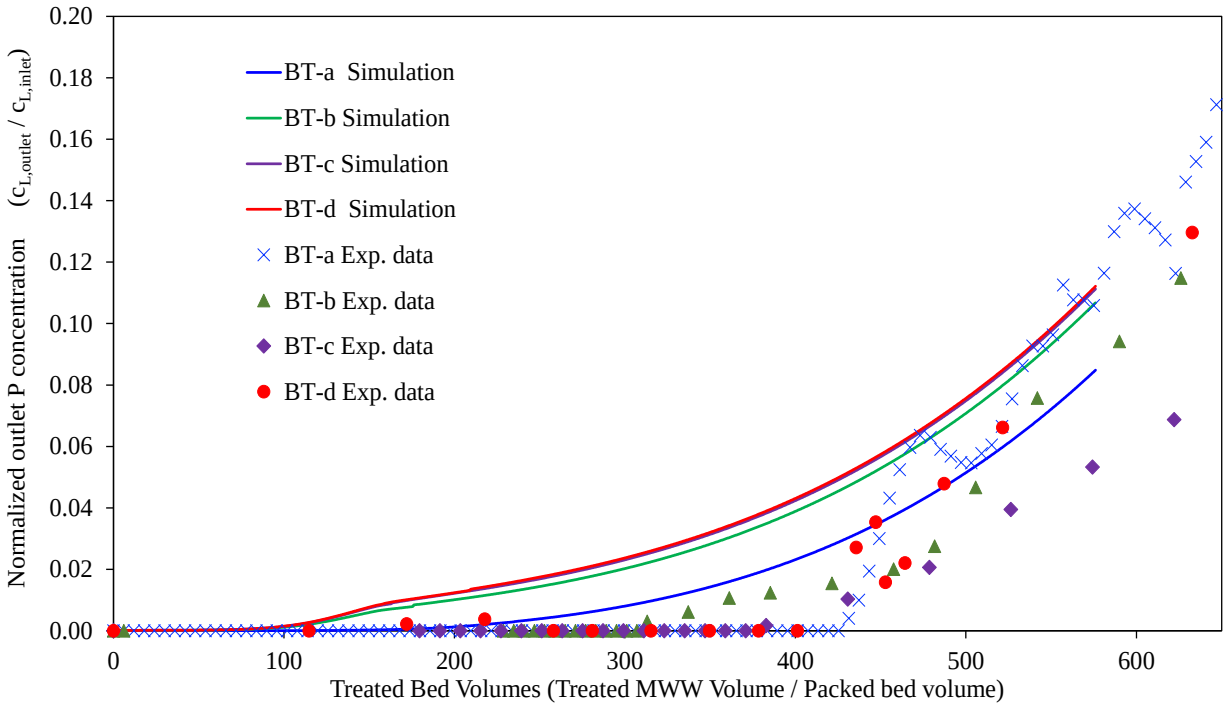

Figure S7. Dimensionless P concentrations at the outlet of the 20-cm packed bed during 4 consecutive adsorption/desorption cycles: experimental data, and predictive simulation conducted with the Aspen Cycle Organizer, with adsorption breakpoint ≤ 0.7 mg L^{-1} and P desorption yield = 95.2% in the first cycle, using the model parameters reported in Tables 2 and 3. Concentrations are normalized by the average feed concentration of phosphate, equal to 7 mg_P L^{-1}.

Table S1
MWW treated bed volumes (BVs) and P sorption capacity at the 10% dimensionless breakpoint, in the benchmark condition (corresponding to Fig. 1) and in the simulations relative to the 6 salinization scenarios described in section 4.4: absolute values and % variation compared to the benchmark condition corresponding to Fig. 1.

Scenario	MWW BVs to reach 10% BP		P sorption capacity @10% BP	
	Absolute value	% variation compared to the baseline scenario	Absolute value	% variation compared to the baseline scenario
Baseline (Table 1, Fig. 1)	552	-	5.17	-
Cl^- inlet conc. 0.30 g/L [a]	474	-14.13%	4.44	-14.11%
Cl^- inlet conc. 0.45 g/L [a]	414	-25.00%	3.88	-25.00%
Cl^- inlet conc. 1.0 g/L [a]	312	-43.48%	2.93	-43.38%
Cl^- inlet conc. 2.0 g/L [a]	180	-67.39%	1.69	-67.25%
SO_4^{2-} inlet conc. 0.24 g/L [a]	456	-17.39%	4.28	-17.35%
SO_4^{2-} inlet conc. 0.38 g/L [a]	396	-28.26%	3.71	-28.29%

[a] The inlet concentrations of all the other anions are equal to those reported in Table 1.

References cited in the Supplementary Material:

T. Kataoka, H. Yoshida, K. Ueyama, Mass transfer in laminar region between liquid and packing material surface in the packed bed, J. Chem. Eng. Jpn. 5 (1972) 132–136. https://doi.org/10.1252/jcej.5.132

E.J. Wilson, C.J. Geankoplis, Liquid Mass Transfer at Very Low Reynolds Numbers in Packed Beds, Ind. Eng. Chem. Fundam. 5 (1966) 9–14. https://doi.org/10.1021/i160017a002

N. Wakao, t: Funazkri, Effect of fluid dispersion coefficients on particle-to-fluid mass transfer coefficients in packed beds: Correlation of sherwood numbers, Chemical Engineering Science, Volume 33, Issue 10, 1978, Pages 1375-1384. https://doi.org/10.1016/0009-2509(78)85120-3